Proceedings of the 1997 IEEE
International Conference on Robotics and Automation
Albuquerque, New Mexico - April 1997

A Systematic Error Analysis of Robotic Manipulators: Application to a High Performance Medical Robot

C. Mavroidis*, S. Dubowsky**, P. Drouet**[1], J. Hintersteiner** and J. Flanz***

* Department of Mechanical and Aerospace Engineering, Rutgers University,
PO Box 909, Piscataway, NJ 08855, USA, Tel 908-445-0732, email: mavro@jove.rutgers.edu

** Department of Mechanical Engineering, Massachusetts Institute of Technology,
Cambridge, MA 02139, USA Tel 617-253-2144

*** Northeast Proton Therapy Center, Massachusetts General Hospital, Boston, MA 02114, USA

Abstract

In this paper, a systematic methodology to calculate the end-effector position and orientation errors of a robotic manipulator is presented. The method treats the physical error sources in a unified manner during the system's design so that the effect they have on the end-effector positioning accuracy can be compared and the dominant sources identified. Based on this methodology, a computer program has been developed that can perform the error analysis on any serial link manipulator. This methodology and the software are applied here to the error analysis of a six degree of freedom high performance medical manipulator.

1 Introduction

In many medical and manufacturing applications of robots, precise end-effector, steady state, positioning accuracy is required. In such applications, even small positioning errors at the manipulator end-effector can have dangerous and costly consequences. Positioning inaccuracies can stem from a number of sources such as structural, measurement and controller errors.

The development of kinematic models, which can account for steady state manipulator errors, is important in evaluating the performance of a robotic system and improving its positioning accuracy. This analysis is important during the design phase in order to verify whether a proposed manipulator design can meet the accuracy requirements of the task. Error models are also important during the manipulator's calibration procedure. Correct identification of the kinematic errors in the model can serve to increase the effectiveness of calibration, and thereby improve the manipulator's positioning accuracy.

Considerable research has been performed in the area of kinematic error analysis, error model derivation, and calibration of robotic manipulators and machine tools [1-4]. Error models have been developed based on screw theory, homogeneous matrices, Denavit and Hartenberg coordinates, and Jacobian matrices [5-9]. Some studies have considered the effects of manipulator joint errors [10, 11], while others were focused on the effects of link dimensional errors [12, 13]. Some generalized methods have been proposed which include non-geometric errors such as thermal effects [14, 15]. Error models have been developed specifically for use in the calibration of manipulators [16, 17]. Researchers have studied methods to predict the error sensitivity of manipulator design [18, 19] and others have done work to find the optimal configurations to reduce the manipulator errors by calibration [20].

In this paper, a systematic methodology to derive the error model of any serial link manipulator is developed. The model can be applied to both the performance evaluation and the calibration of the manipulator, incorporating any type of physical error sources that may exist, such as geometric errors, backlash, joint or link deflections. The method treats the physical error sources in a unified manner during the system's design so that the effect they have on the end-effector positioning accuracy can be compared and the dominant sources identified. Based on this methodology, an error analysis software package has been constructed which uses a combination of symbolic and numeric computations to calculate the error model for any six degree of freedom serial link manipulator.

This error methodology and computer program have been applied to the performance evaluation of a robotic manipulator to be used in a new important medical application. The Northeast Proton Therapy Center (NPTC) is now being constructed at the Massachusetts General Hospital (MGH) [21, 22]. This cancer research and treatment facility will have a new advanced proton therapy system. The NPTC is scheduled to begin operations with patients in 1998. A major component of the system is its robotic patient positioning system (PPS). This system will automatically position a patient in a proton beam that emanate from a "nozzle" located on a rotating gantry ring structure. The required absolute positioning accuracy of the PPS is ±0.5 mm. Larger errors may be dangerous to the patient [23]. It should be noted that constraints of the medical environment prevent the use of real-time end-point measurements that might in other cases be used to correct for static end-point errors. Hence the inherent accuracy of the system is critical. As it is described in Section 5, the methodology and software developed in this paper, are being used to evaluate the PPS design. The same method will also be used in the future in the error calibration procedure and the development of real time error compensation algorithms.

1. Visiting graduate student from the Laboratoire de Robotique de Paris, 10-12 Avenue de l'Europe, Velizy, France.

0-7803-3612-7-4/97 $5.00 © 1997 IEEE

2 Kinematic Model Without Errors

Classical kinematic analysis of a manipulators requires the definition of reference frames at the manipulator base, end-effector, and at each of the joints [24]. For a six degree of freedom manipulator, 7 reference frames F_i (i ranging from 0 to 6) are defined, such as shown in Figure 1. Generally, these frames are characterized using the Denavit and Hartenberg method [24]. The position and orientation of a reference frame F_i with respect to the previous reference frame F_{i-1} is defined with a 4x4 matrix $\mathbf{A}_i$ that has the general form:

$$\mathbf{A}_i = \begin{pmatrix} \mathbf{R}_i & \mathbf{T}_i \\ 0 & 1 \end{pmatrix} \quad (1)$$

The $\mathbf{R}_i$ term is a 3x3 orientation matrix composed of the direction cosines of frame F_i with respect to frame F_{i-1} and $\mathbf{T}$ is a 3x1 vector of the coordinates of center O_i of frame F_i in F_{i-1}. (Bold lettered variables represent vectors or matrices.) The elements of matrices $\mathbf{A}_i$ depend on the geometric parameters of the manipulator and the manipulator configuration parameters $\mathbf{q}$. For a 6R manipulator, $\mathbf{q}$ is composed of the six manipulator joint angles.

The position and orientation of the end-effector frame F_6, with respect to the inertial reference frame F_0, is represented by the homogeneous matrix $\mathbf{A}_T$. The elements of $\mathbf{A}_T$ depend on the 3 position and 3 orientation parameters of frame F_6, with respect to frame F_0. These parameters are also represented with a 6x1 vector $\mathbf{X}_T^i$. At this point the superscript i will be added to X_T to denote the ideal position of F_6 with respect to frame F_0, if no errors exist in the manipulator. The superscript r, will be used later to denote the real or actual position of F_6 when errors exist. The matrix $\mathbf{A}_T$ is formed by multiplying all of the $\mathbf{A}_i$ matrices [24]:

$$\mathbf{A}_T = \mathbf{A}_1\mathbf{A}_2 \ldots\ldots \mathbf{A}_6 \quad (2)$$

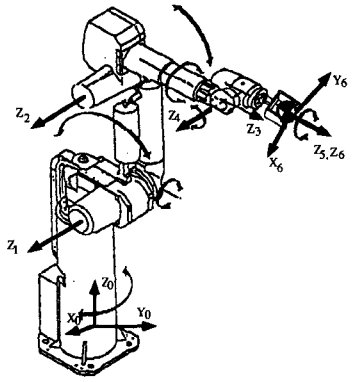

Figure 1: GMF - a 6R industrial manipulator

From Equation (2), known as the "loop closure equation," six scalar equations are obtained to calculate the end-effector coordinates $\mathbf{X}_T^i$ when the configuration parameters $\mathbf{q}$ are known:

$$\mathbf{X}_T^i = \mathbf{f}^i(\mathbf{q}, \mathbf{s}) \quad (3)$$

The vector $\mathbf{f}^i$ is a non-linear function of the configuration parameters, $\mathbf{q}$, and a vector of the manipulator structural parameters $\mathbf{s}$. Equation (3) represents the relationship between the manipulator's configuration parameters and the position and orientation coordinates of its end-effector. This is known as the "direct kinematic model." This model is often used in a manipulator controller to calculate the end-effector inertial coordinates from system joint displacements. A "manipulator inverse kinematic model" is used to calculate the configuration parameters to achieve a desired end-effector location and orientation.

If the manipulator has errors, Equation (3) will not accurately represent the system's direct kinematics. Using equation (3) to position the manipulator end-effector, the manipulator would placed it in a different position then the desired one. In the following section, equations are formulated to accurately represent the relationship between configuration parameters $\mathbf{q}$ and end-effector coordinates $\mathbf{X}_T$ when errors exist in the manipulator.

3 Manipulator Error Classification

3.1 The physical errors

There are many possible sources of errors in a manipulator. These errors are referred to as "physical errors", to distinguish them from "generalized errors" which are defined later. The main sources of physical errors in are:

- **Machining errors:** These errors are resulting from machining tolerances of the individual mechanical components that are assembled to build the robot.
- **Assembly:** These errors include linear and angular errors that are produced during the assembly of the various manipulator mechanical components.
- **Deflections:** Link and joint flexibility can cause elastic deformations of the structural members of the manipulator, resulting in large end-effector errors, especially in long reach manipulator systems. Local material deformations can also be another source of end-effector errors.
- **Measurement and Control:** Measurement, actuator, and control errors will create end-effector positioning errors. The resolution of encoders and stepper motors are examples of such errors.
- **Joint errors:** These include bearing run-out errors in rotating joints and rail curvature errors in linear joints.
- **Clearances:** Backlash errors can occur in the motor gear box and in the manipulator joints.

In most cases, the physical errors are usually very small. However, they can be amplified by the system to cause large errors at the end-effector. As a result, it is essential to identify those errors in the system which significantly influence the end-effector positioning accuracy.

3.2 Types of errors

Errors can be distinguished into "repeatable" and "random" errors [25]. Repeatable errors are errors whose numerical value and sign are constant for each manipulator configuration. An example of a repeatable error is an assembly error. Random errors are errors whose numerical value or

sign changes unpredictably. At each manipulator configuration, the exact magnitude and direction of random errors cannot be uniquely determined, but only specified over a range of values. An example of a random error is the error that occurs due to backlash of an actuator gear train.

3.3 The generalized errors

Physical errors change the geometric properties of a manipulator. As a result, the frames defined at the manipulator joints are slightly displaced from their expected, ideal locations. In Figure 2, frame F_i is shown in the ideal location F_T^i and in its real location F_T^r due to errors.

The position and orientation of a frame F_T^r with respect to its ideal location F_i^i is represented by a 4x4 homogeneous matrix $\mathbf{E}_i$. The rotation part of matrix $\mathbf{E}_i$ is the result of the product of three consecutive rotations e_{si}, e_{ri}, e_{pi} around the Y, Z and X axes respectively. (These are the Euler angles of F_T^r with respect to F_T^i.) The subscripts s, r, and p represent spin (yaw), roll, and pitch, respectively. The translational part of matrix $\mathbf{E}_i$ is composed of the 3 coordinates e_{xi}, e_{yi} and e_{zi} of point O_T^r in F_T^i.

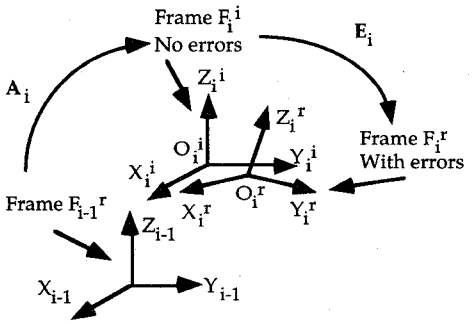

Figure 2: Frame displacement due to errors

The 6 parameters e_{xi}, e_{yi}, e_{zi}, e_{si}, e_{ri} and e_{pi} are called here "generalized error" parameters. For a six degree of freedom manipulator, there are 36 generalized errors which can be written in vector form as ε=[...,e_{xi}, e_{yi}, e_{zi}, e_{si}, e_{ri}, e_{pi},..], with i ranging from 1 to 6. Since the physical errors are small, the generalized errors e_{xi}, e_{yi}, e_{zi}, e_{si}, e_{ri} and e_{pi} are also small, so a first order approximation can be applied to their trigonometric functions and products. Matrix $\mathbf{E}_i$, after the first order approximation, has the form:

$$\mathbf{E}_i = \begin{pmatrix} 1 & -e_{ri} & e_{si} & e_{xi} \\ e_{ri} & 1 & -e_{pi} & e_{yi} \\ -e_{si} & e_{pi} & 1 & e_{zi} \\ 0 & 0 & 0 & 1 \end{pmatrix} \quad (4)$$

The generalized errors are easily calculated from the physical errors.

4 Error Analysis Method

The end-effector position and orientation error $\Delta\mathbf{X}$ is defined as the 6x1 vector that represents the difference between the real position and orientation of the end-effector and the ideal or desired one:

$$\Delta\mathbf{X} = \mathbf{X}_T^r - \mathbf{X}_T^i \quad (5)$$

Here, $\mathbf{X}_T^r$ and $\mathbf{X}_T^i$ are the 6x1 vectors that represent the position and orientation of the end-effector reference frame (F_6) in the inertial reference system (F_0) for the real and ideal case, respectively. The vector $\Delta\mathbf{X}$ must be calculated for a given set of physical errors. Many physical errors may not play an important role in end-effector error. The first step in this analysis is to determine which physical errors significantly influence the end-effector positioning accuracy. A manipulator error model, which maps the manipulator's physical errors into generalized error components, and then into end-effector errors is used. If the end-effector error is greater than the desired tolerance, the identified physical errors can either be corrected or the manipulator controller can be programmed to compensate for the errors if the errors are repeatable. A complete discussion of these compensation algorithms is beyond the scope of this paper. In this section, a general method to obtain the error model is described.

4.1 Kinematic model with errors

When the generalized errors are considered in the model, the manipulator loop closure equation takes the form:

$$\mathbf{A}_T = \mathbf{A}_1\mathbf{E}_1\mathbf{A}_2\mathbf{E}_2.....\mathbf{A}_6\mathbf{E}_6 \quad (6)$$

As in Section 2, the end-effector inertial coordinates, $\mathbf{X}_T^r$=(x_T^r, y_T^r, z_T^r), can be calculated from Equation (6):

$$\mathbf{X}_T^r = \mathbf{f}^r(\mathbf{q}, \varepsilon, \mathbf{s}) \quad (7)$$

Here, $\mathbf{f}$ is a vector non-linear function of the configuration parameters $\mathbf{q}$, the vector of the generalized errors ε, and the vector of the structural parameters $\mathbf{s}$. Equation (7) is called the "direct kinematic error model" and can be used in the manipulator controller to calculate the real end-effector inertial coordinates from system joint displacements when errors exist in the manipulator.

In the error analysis of a manipulator, the end-effector position and orientation errors are calculated as a function of the generalized errors. This is required to understand the effect of the physical errors on the end-effector positioning accuracy. Since the generalized errors are small, $\Delta\mathbf{X}$ can be calculated by the following linear equation in ε:

$$\Delta\mathbf{X} = \mathbf{J}_e\,\varepsilon \quad (8)$$

Here, $\mathbf{J}_e$ is the 6x36 Jacobian matrix of the function $\mathbf{f}^r$ defined in Equation (7) with respect to the elements of the generalized error vector ε. Equation (8) is called the "manipulator error model". The elements of $\mathbf{J}_e$ are:

$$\mathbf{J}_e[i,j] = \frac{\partial \mathbf{f}[i]}{\partial \varepsilon[j]} \quad (9)$$

where i ranges from 1 to 6 and j ranges from 1 to 36. Matrix $\mathbf{J}_e$ is called the "manipulator error matrix."

4.2 Symbolic calculation

A computer program has been developed to calculate the manipulator error model and perform the error analysis of any serial link manipulator. The manipulator error matrix is calculated analytically using the symbolic calculation software package *Maple* [26]. The inputs to the program

are homogeneous matrices $\mathbf{A}_i$ that represent the manipulator's nominal geometry. The output of the *Maple* program is a C script containing the analytical algebraic forms of the error matrix $\mathbf{J}_e$. Then, a *Matlab* program [27] reads the input files that define the numerical values of the configuration parameters $\mathbf{q}$, the generalized errors ε, and the structural parameters $\mathbf{s}$ and executes the C-script file that contains the numerical value of $\mathbf{J}_e$. From Equation (8), the treatment point error vector $\Delta\mathbf{X}$ is calculated.

5 Application to the PPS

5.1 The Patient Positioning System

A schematic of the MGH PPS is shown in Figure 3. It is a six degree of freedom manipulator being designed by General Atomics [28, 29]. The first three joints are prismatic. The maximum travel for these joints is 90" for the lateral (X) axis, 24" for the vertical (Y) axis, and 58" for the longitudinal (Z) axis. The last three joints are revolute joints. The first revolute joint has an axis of rotation parallel to the Y axis and can rotate ±95°. The last two joints are used for small corrections around an axis of rotation parallel to the Z (i.e. roll) and X (i.e. pitch) axes, respectively, and have a maximum rotation angle of ±3°. All of the joints are actuated by stepper motors. The connecting members and supporting structures of the PPS are made out of steel. The manipulator's "end-effector" is a couch which supports the patient in a supine position.

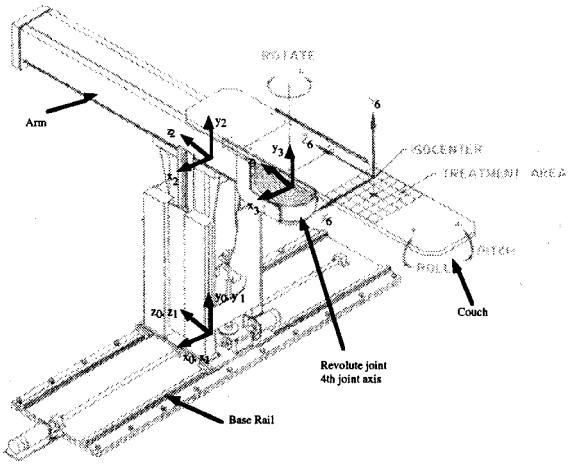

Figure 3: The patient positioning system [28]

In Figure 3, some of the reference frames are shown. F_0 is the fixed base inertial reference system. F_1 moves with the first linear joint in the X direction, and is aligned with F_0 in the zero position. F_2 moves with the top of the second linear joint in the Y direction. F_3 moves with the end of the third linear joint in the Z-direction. F_6 is the reference system defined at the treatment point, such as a tumor in the patient's body.

5.2 Single error analysis

A large set of potential physical error sources has been identified for the PPS design. An error model has been calculated using the method and the program presented in Section 4. For each physical error, the treatment point error has been calculated. This was performed in order to determine which physical errors induce large treatment errors. It was found that the angular treatment point errors resulting from the physical errors considered were very small from a medical point of view and could therefore be ignored. However, the linear displacement error induced by some physical errors was found to be very significant. The amplification of small physical errors into large treatment point errors is primarily caused by the long cantilever utilized in the design of this system. In this section, examples of these errors are presented.

- **Base rail curvature**

The first three joints of the PPS are prismatic joints, for which the moving elements slide on rails. The base rail is considered in this example (see Figure 3.) One of the possible physical errors associated with the base rail is the curvature of the rail around the Y_0 axis. This is a repeatable error. A representation of the rail error is shown in Figure 4. The error is assumed to be a sinusoidal function of the travel d_1 of the prismatic joint. The rail has a maximum angular deviation of 0.000125 radians and a maximum linear error of 0.2 mm over its total length.

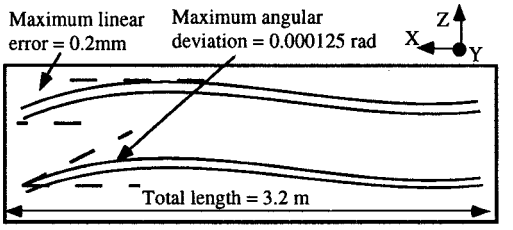

Figure 4: Base rail curvature error of the PPS

The generalized errors associated with these physical error are found to be:

$$e_{z1} = -0.000062\, d_1 - 0.060706 \sin\left(\frac{\pi}{1600\, d_1}\right)$$

$$e_{s1} = -0.000062\, d_1 - 0.000119 \cos\left(\frac{\pi}{1600\, d_1}\right)$$

In Figure 5, the treatment point error for the rail error source is shown for Z and X directions. For this particular physical error, there is no error in the Y direction. These treatment point errors are calculated over the span of the manipulator workspace, which is defined as the range of motions which will keep the proton beam within the treatment volume. The treatment volume is a 50x50x20 cm volume on the couch within which the treatment point must be located. The maximum treatment point error due to base rail curvature is 0.22 mm in the X direction and 0.08 mm in the Z direction. This error is considered to be significant because, in some configurations, almost 50% of the total accuracy specification is reached by just this error alone. However it is a repeatable error, so that the system software can compensate for it if it can be well characterized.

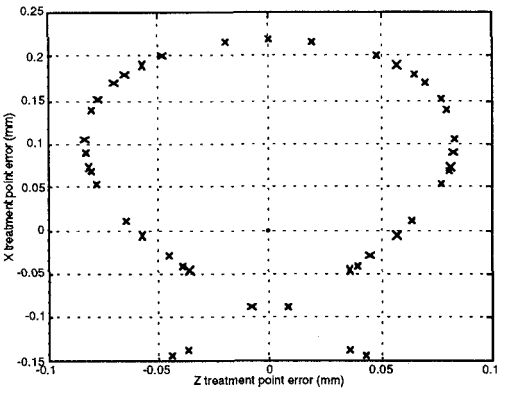

Figure 5: Effect of base rail curvature

- **Deflections - Elastic deformations**

Deflections and elastic deformations of various structural members of the PPS are another significant source of errors. Deflections of the arm, vertical post, and couch (see Figure 3,) along with elastic deformations of the bearings, rails, and lead screws can occur. In this example, the deflection of the arm is studied. This is a repeatable error. The arm was modeled as an elastic beam. From classical beam theory [30], the corresponding generalized errors have been calculated as functions of the configuration parameters. Using the error model of the PPS, the treatment error is calculated over the manipulator workspace.

The results of this calculation are shown in a three dimensional diagram in Figure 6. The maximum error is 0.12 mm in the X direction, 0.44 mm in the Y direction, and 0.25 mm in the Z direction. These results show that the deflection of the PPS structural members are major sources of inaccuracy. Based on these results, the addition of a load cell to the PPS design has been decided. The load cell will be mounted at the end of the PPS arm. The measurements from the load cell will be used in a deflection compensation algorithm.

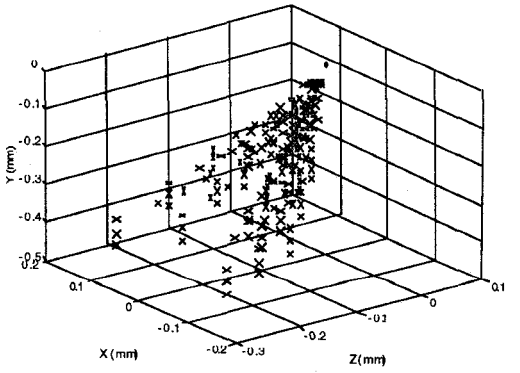

Figure 6: Effect of deflections of the arm

5.3 Combined error analysis

Figure 7 shows the treatment point error calculation where the identified physical errors are assumed to be present. Repeatable errors have been summed arithmetically, assuming that the sign of the errors is known. A root mean square sum (RMS) has been used for random errors. It was found that an uncalibrated PPS will have a maximum positioning error of 5.48 mm, as defined by the radius of the sphere that includes all of the treatment point errors shown in Figure 7. This error is significantly greater than the maximum allowable tolerance of ±0.5 mm. However, many repeatable errors can be corrected by using a compensation algorithm. It is assumed that a correction algorithm can be developed which will largely correct for repeatable errors. Based on some calculations, it has been estimated that due to uncomplete compensation of repeatable errors the residual accuracy of the PPS becomes ±0.25 mm. Random errors cannot be corrected. The RMS sum of all random was calculated to be ±0.1 mm. Total prediction of the system absolute accuracy is ±0.35mm.

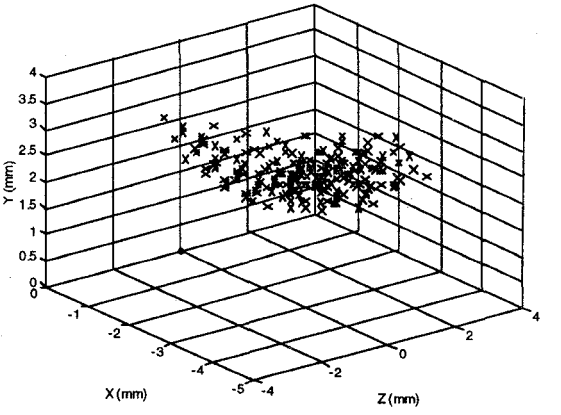

Figure 7: Sum of the treatment point errors

Since the PPS is currently in the design stage, all of the values used in the analysis were based upon specifications developed from the "paper design." These values, however, may not completely reflect the actual behavior of the PPS when it is constructed and installed. Measurements of the significant physical errors will need to be made when the system is installed.

6 Conclusions

In this paper, a systematic methodology to calculate a manipulator error model is presented. Based on this methodology, a computer program has been developed which can perform an error analysis on any serial link manipulator. This methodology and software were used in the error analysis of a six degree of freedom manipulator which will be used in a medical robot for cancer treatment and research at the Massachusetts General Hospital.

It was found that the uncalibrated system has a maximum positioning error of ±5.28 mm, which is significantly larger than the required accuracy of ±0.5 mm. However, a calibration procedure for this system, based on the analysis presented here, will reduce the treatment point error to ±0.35 mm, which meets the accuracy specification.

7 Acknowledgments

The support of this project by the Northeast Proton Therapy Center of the Massachusetts General Hospital is acknowledged. The support of NASA for the development of some of the fundamental methodology is acknowledged. The authors would especially like to thank Dr. Michael Goitein for his comments. The information provided by General Atomics is also acknowledged.

8 References

1. Veitchegger W. and Wu C., "Robot Accuracy Analysis Based on Kinematics," *IEEE Journal of Robotics and Automation*, Vol. RA-2, No-3, pp. 171-179., 1986.

2. Hollerbach J., "A survey of kinematic calibration," *Robotics Review*, Khatib O. et al editors, Cambridge, MA; MIT Press, 1988.

3. Mooring B., Roth Z., and Driels M., *Fundamentals of Manipulator Calibration*, New York; John Willey & Sons, 1991.

4. Kirdena V. and Ferreira P., "Mapping the Effects of Positioning Errors on the Volumetric Accuracy of Five-Axis CNC Machine Tools," *Intern. J. of Machine Tools in Manufacturing*, Vol. 33, No. 3, pp. 417-437, 1993.

5. Ziegert J., Olson D., Datseris P., "Description of Machine Tool Errors Using Screw Coordinates," *Trans. of the ASME, J. of Mech. Design*, Vol. 114, pp. 531-535, 1992.

6. Wu C., "A Kinematic CAD Tool for the Design and Control of a Robot Manipulator," *The Intern. J. of Rob. Research*, Vol. 3, No. 1, pp. 58-67, 1984.

7. Chen J. and Chao L., "Positioning Analysis for Robot Manipulators With All Rotary Joints," *Proceedings of the 1986 IEEE Robotics and Automation Conference*, Vol. 2, pp. 1011-1016, 1986.

8. Lin P. and Ehmann K., "Direct Volumetric Error Evaluation for Multi-Axis Machines," *International Journal for Machine Tools in Manufacturing*, Vol. 33, No. 5, pp. 675-693, 1993.

9. Mirman C. and Gupta K., "Identification of Position Independent Robot Parameter Errors Using Special Jacobian Matrices," *International Journal of Robotics Research*, Vol. 12, No. 3, pp. 288-298, 1993.

10. Benhabib B., Fenton R. and Goldenberg A., "Computer-Aided Joint Error Analysis of Robots," *IEEE J. of Rob. and Autom.* Vol. RA-3, No. 4, pp. 317-322, 1987.

11. Waldron K. and Kumar V., "Development of a Theory of Errors for Manipulators," *Proceedings of the Fifth World Congress on the Theory of Machines and Mechanisms*, pp. 821-826, 1979.

12. Ferreira P. and Liu R., "An Analytic Quadratic Model for the Geometric Error of A Machine Tool," *Journal of Manufacturing Systems*, Vol. 5, No. 1, pp. 51-62.

13. Vaichav R. and Magrab E., 1987, "A General Procedure to Evaluate Robot Positioning Errors," *The Intern. J. of Rob. Research*, Vol. 6, No. 1., pp. 59-74.

14. Donmez M., Liu C. and Barash M., "A Generalized Mathematical Model for Machine Tool Errors," *ASME Publications: Modeling, Sensor and Control in Manufacturing Processes*, pp. 231-243, 1988.

15. Soons J., Theus F. and Schellekens P., "Modelling the Errors of Multi-axis Machines: A General Methodology," *Precision Engineering*, Vol. 14, No. 1, pp. 5-19, 1992.

16. Broderick P. and Cirpa R., "A Method for Determining and Correcting Robot Position and Orientation Errors Due to Manufacturing," *Transactions of the ASME, Journal of Mechanisms, Transmissions and Automation in Design*, Vol. 110, pp. 3-10, 1988.

17. Zhuang H., Roth Z. and Hamano F., "A Complete and Parametrically Continuous Kinematic Model for Robot Manipulators," *IEEE Transaction in Robotics and Automation*, Vol. 8, No. 4, pp. 451-462, 1992.

18. Cleghorn W., Fenton R. and Fu J., "Optimum Tolerancing of Planar Mechanisms Based on an Error Sensitivity Analysis," *Transactions of the ASME, Journal of Mechanical Design*, Vol. 115, pp. 306-313, 1993.

19. Ting K. and Long Y., "Performance Quality and Tolerance Sensitivity of Mechanisms," *Trans. of the ASME, J. of Mech. Design*, Vol. 118, pp. 144-150, 1996.

20. Zhuang H., Wang K. and Roth Z., "Optimal Selection of Measurement Configurations for Robot Calibration Using Simulated Annealing," *Proceedings of the IEEE 1994 International Conference in Robotics and Automation*, pp. 393-398, San Diego, CA, 1994.

21. Flanz J. et al., "Overview of the MGH-Northeast Proton Therapy Center plans and progress," *Nuclear Instruments and Methods in Physics Research B*, Vol. 99, pp. 830-834, 1995.

22. NPTC, Web Page of the Northeast Proton Therapy Center at the Massachusetts General Hospital, http://www.mgh.harvard.edu/depts/nptc.htm, 1996.

23. Rabinowitz I. et al, "Accuracy of Radiation Field Alignment in Clinical Practice," *International Journal of Radiation Oncology, Biology and Physics*, Vol. 11, pp. 1857-1867, 1985.

24. Craig J., *Introduction to Robotics: Mechanics and Control*, Addison Willey, 1989.

25. Slocum A., *Precision Machine Design.*, Englewood Cliffs, 1992.

26. Waterloo Maple, Inc., *Maple V Release 3.* 1981-95.

27. The Mathworks, Inc., *Matlab 4.2c.1.* 1984-94.

28. General Atomics Patient Positioner Preliminary Design Documents, 1995.

29. Flanz J., et al., "Design Approach for a Highly Accurate Patient Positioning System for NPTC," *Proceedings of the PTOOG XXV and Hadrontherapy Symposium*, Belgium, September, 1996.

30. Crandall S., Dahl N. and Lardner T., *An Introduction to the Mechanics of Solids*, McGraw-Hill, 1978.